

# Glucose-Sensitive Nanoparticles for Controlled Insulin Delivery

Todd C. Zion, Henry H. Tsang, and Jackie Y. Ying\*  
Department of Chemical Engineering, Massachusetts Institute  
of Technology, Cambridge, MA 02139-4307

**Abstract**—A novel reverse microemulsion (RM) mediated synthesis of glucose-responsive nanoparticles was developed for controlled insulin delivery. Nanoparticles were constructed using a model system comprised of dextran, poly( $\alpha$ -1,6 glucose), physically crosslinked with the tetrafunctional glucose-binding protein, Con A. A rapid-screening technique was used to quantify RM phase behavior in the presence of dextran, Con A and insulin. The extent of the RM existence region diminishes with increasing dextran and Con A concentrations and with increasing dextran molecular weight. Crosslinking efficiency between Con A and fluorescein isothiocyanate dextran (FITC-Dex) was found to depend on the total concentration of Con A as well as the ratio of Con A to FITC-Dex. Functionalizing dextran with higher affinity mannose ligands and increasing dextran molecular weight both improved crosslinking efficiency. The nanoparticles dissolved when dispersed in buffered saline solutions containing elevated glucose concentrations and were most responsive within the physiological range. Finally, insulin was encapsulated in select formulations and found to release preferentially at these elevated glucose concentrations.

**Index Terms**—Nanoparticles, drug delivery, insulin, reverse microemulsion.

## I. INTRODUCTION

DEVELOPING alternative or more convenient methods for administering proteins is currently an intense area of research. In the case of insulin for the treatment of diabetes mellitus, current dosage regimens that maintain acceptably low serum glucose levels comprise of up to four subcutaneous injections per day [1]. Compliance with such demanding regimens is difficult, making very attractive the development

of a means to either reduce the number of injections or facilitate administration through non-invasive routes such as oral or pulmonary delivery.

Polymer nanoparticles have shown promise in addressing these challenges by first providing a means to encapsulate the protein and release it over extended periods of time, thereby potentially reducing the dosage frequency. In addition, it has been demonstrated that protein encapsulation within certain polymers provides protection from proteolytic enzymes to facilitate oral delivery [2-4]. Furthermore, it was shown that small (submicron) colloidal particles are absorbed and transported through the intestinal mucosa [5-7], thereby enhancing protein oral bioavailability. It is known that particles delivered to the lung are preferentially within the size range of 500 nm – 3.3  $\mu$ m to deposit in the alveoli [8]. Systemically absorbed nanoparticles may also avoid rapid elimination due to macrophage digestion provided the size is less than about 300 nm [9].

Despite the attractive features of nanoparticles in enhancing insulin delivery, the usual mechanism of sustained release is independent of physiological blood sugar concentration. The best way to treat diabetes, however, is to provide exogenous insulin proportional to the varying blood glucose level in the patients [10]. Toward such an end, several researchers have attempted to develop glucose-responsive materials. In particular, those based on competitive binding have received considerable attention [11, 12]. In one such system, a polymer comprising covalently bound sugar is crosslinked using a multifunctional glucose-binding protein such as one of the plant lectins [13, 14]. When the matrix comes in contact with free glucose in solution, the protein releases polymeric glucose and binds to free glucose molecules, causing the hydrogel to disintegrate. Nanoparticles constructed from such glucose-responsive materials might then not only improve the means of insulin delivery as outlined above but also provide a more desirable release profile once administered.

Our laboratory has recently developed a reverse microemulsion (RM) synthesis of inorganic nanoparticles for catalytic applications [15] and sought to apply this technique to the synthesis of polymer nanoparticles for controlled drug delivery. RM's are spontaneously forming, thermodynamically stable, dispersed systems having a uniform particle size in the

\* To whom correspondence should be addressed

Manuscript received November 8, 2002. This work was supported by the Singapore-MIT Alliance (MEBCS Programme) and the National Science Foundation (CTS-0118705).

T. C. Zion is with the Department of Chemical Engineering, Massachusetts Institute of Technology, Cambridge, MA 02139 USA (e-mail: tzion@mit.edu).

H. H. Tsang is with the Department of Chemical Engineering, Massachusetts Institute of Technology, Cambridge, MA 02139 USA (e-mail: hhtsang2001@yahoo.com).

J. Y. Ying is with the Department of Chemical Engineering, Massachusetts Institute of Technology, Cambridge, MA 02139 USA (phone: 617-253-2899; fax: 617-452-3436; e-mail: jyying@mit.edu).

range of 5-200 nm. These structural characteristics make RM's an ideal medium for the controlled synthesis of ultrafine particles. The specific goals of this project are to apply RM's to the synthesis of glucose-sensitive nanoparticles for controlled insulin delivery. The model system investigated is based on the competitive binding of the jack-bean lectin Concanavalin A (Con A) with dextran, a biocompatible and biodegradable polymer of glucose containing predominantly linear  $\alpha$ -1,6 glucosidic linkages with varying degrees of  $\alpha$ -1,3-linkage branching [16].

## II. EXPERIMENTAL

### A. Materials

Dextrans and FITC-labeled dextrans of various molecular weights, Con A (Type V), Insulin from Bovine Pancreas, Tween 80, and Span 80 were purchased from Sigma-Aldrich (Milwaukee, WI). Captex 355 (C<sub>8</sub>/C<sub>10</sub> triglycerides) and Capmul MCM (C<sub>8</sub>/C<sub>10</sub> mono-/di-glycerides) were generously donated by Abitec Corporation (Janesville, WI). Zn<sup>2+</sup>-free insulin was prepared according to a previously published procedure [17]. Mannosylated FITC-dextran was prepared using the divinylsulfone procedure described previously [18].

### B. Microemulsion Ternary Diagram Construction

The existence of RM's is identified by preparing various pseudoternary compositions and evaluating the optical clarity of the mixture. Clear, transparent formulations are indicative of stable RM's as the size of the aqueous domains are much smaller than the wavelength of light [19]. To quantify the optical clarity of a particular system at a number of compositions and temperatures while minimizing the experimental time and materials required, a rapid screening approach was developed. Briefly, varying amounts of surfactant (3:2 w/w Tween 80/Span 80) and oil (3:1 w/w Captex 355/Capmul MCM) were micropipetted into a glass, flat-bottomed, 96-well microplate (500- $\mu$ l well capacity, Alltech, Deerfield, IL) and mixed thoroughly. The appropriate amount of aqueous solution was then added to make a total volume of 350  $\mu$ l and mixed again in such a way that each well contained a specific ternary composition. Each composition was run in duplicate, and absorbance values for all 96 wells were collected at a wavelength of 450 nm using a VERSAmax microplate reader (Molecular Devices, Sunnyvale, CA) to quantify turbidity. The internal plate-reader thermal incubator was then adjusted to take absorbance readings of plates equilibrated at elevated temperatures.

The data resulting from such experiments was plotted on a pseudoternary contour diagram thereby yielding a pseudoternary surface, while pseudoternary surfaces plotted as a function of temperature yield a prism. To evaluate the effect of dissolved proteins and polymers on reverse microemulsion phase behavior, varying concentrations of each component were dissolved in the aqueous phase before addition to the surfactant/oil mixture. In this way, the RM existence region

was identified as a function of the type and concentration of aqueous dissolved species.

### C. Dynamic Light Scattering (DLS) Measurements

A Brookhaven Instruments Photon Correlation Spectrometer model BI-9000 AT (Holtsville, NY) equipped with an argon ion laser model Stabilite 2017 from Spectra-Physics (Mountain View, CA) was used. Light Scattering was monitored at 90° angle and 25°C with polystyrene beads used as a standard. The particle size and size distribution were obtained by non-negatively constrained least squares fitting of the autocorrelation function. Kinematic viscosity measurements were obtained using a falling ball viscometer (VWR, Boston, MA) with a constant of 0.04231 cSt/s. Multiplying this value by the density gives the viscosity in cP. An Abbe refractometer (American Optical, Buffalo, NY) was used to determine the refractive index. Both viscosity and refractive index values are required in order to determine the hydrodynamic diameter from the measured diffusion coefficient according to the Stokes-Einstein equation.

### D. Nanoparticle Synthesis

Glucose-sensitive nanoparticles were prepared using a RM formulation comprising 65% v/v oil (3:1 w/w Captex 355/Capmul MCM), 25% v/v surfactant (3:2 w/w Tween 80/Span 80), and 10% v/v aqueous phase. Dextran, covalently modified with fluorescein isothiocyanate (FITC-Dex), was chosen as the crosslinking polymer such that the extent of crosslinking due to Con A and the extent of particle dissolution could be monitored by fluorescence spectroscopy. To 1.8 ml of a premixed solution of oil and surfactant, 160  $\mu$ l of a 0.1 N HCl solution containing Con A and FITC-Dex of predetermined concentrations was added and mixed thoroughly. Next, 20  $\mu$ l of a pH 7.0 200 mM BES buffered saline solution containing 1 M NaCl and 20 mM MnCl<sub>2</sub> and CaCl<sub>2</sub> and 20  $\mu$ l of a 1 N NaOH solution were added in succession to neutralize the pH and activate Con A/dextran crosslinking. The parameters explored in this study were aqueous concentrations of Con A and FITC-Dex as well as FITC-Dex MW. In addition, we also studied the effect of dextran mannosylation. Insulin was incorporated in the aqueous phase of select compositions at a concentration of 20 mg/ml to determine the encapsulation efficiency and glucose-sensitive release.

### E. Particle Isolation and Characterization

The particle-containing microemulsions were diluted 1:10 (v/v) with ethanol and centrifuged for 30 minutes to separate the particles from the ethanol, oil and surfactant. The centrifuge cake was redispersed by sonication and washed twice in ethanol to remove residual oil and surfactants, followed by washing with 20 mM pH 7.0 BES buffered saline solution to remove any unbound dextran. The remaining material was redispersed in ethanol by sonication and dried under vacuum at room temperature for SEM viewing (FEI/Philips XL30 FEG ESEM).

### F. In vitro Release Studies

The particles isolated from each experiment according to the procedure above were redispersed in a known volume of pH 7.0 BES buffer containing 0.150 M NaCl and 1 mM  $Mn^{2+}$  and  $Ca^{2+}$  ions. The dispersion was then split into a control half and an experimental half. The control half was diluted with a blank buffer solution while the experimental half was diluted with a glucose-containing buffer solution. Both dispersions were mixed for 30 minutes at 25°C, followed by centrifugation for 30 minutes to separate the particles from the aqueous medium. Half the volume was collected for analysis and replaced with blank buffer for the control or a higher concentration glucose buffer for the experiment. The collected samples were analyzed using an *f*max fluorescence spectrophotometer (Molecular Devices; Sunnyvale, CA) with  $\lambda_{ex} = 485$  nm and  $\lambda_{em} = 538$  nm to determine the amount of dextran dissolved from the particles after each step. The results provide a measure of glucose-sensitive particle dissolution (i.e. the difference between the values obtained for the experiment and control) for a large number of compositional variations. However, such a technique does sacrifice an understanding of the true kinetics of polymer release, a subject for future experiments.

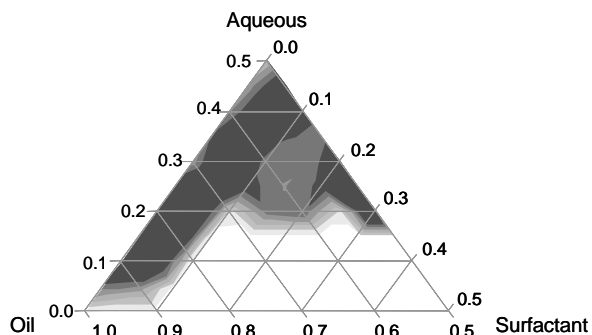
The extent of dextran crosslinking for each formulation was determined by comparing the amount of dextran released after complete dissolution to the amount initially loaded into the RM. The concentration of released insulin was determined by high-performance liquid chromatography (HPLC) using a C18 column (Waters Symmetry 5 mm C18, 250 × 4.6 mm) and a mobile phase of 1.4 ml/min containing 37% v/v acetonitrile in a pH 2.4 sodium sulphate/phosphoric acid buffer.

## III. RESULTS AND DISCUSSION

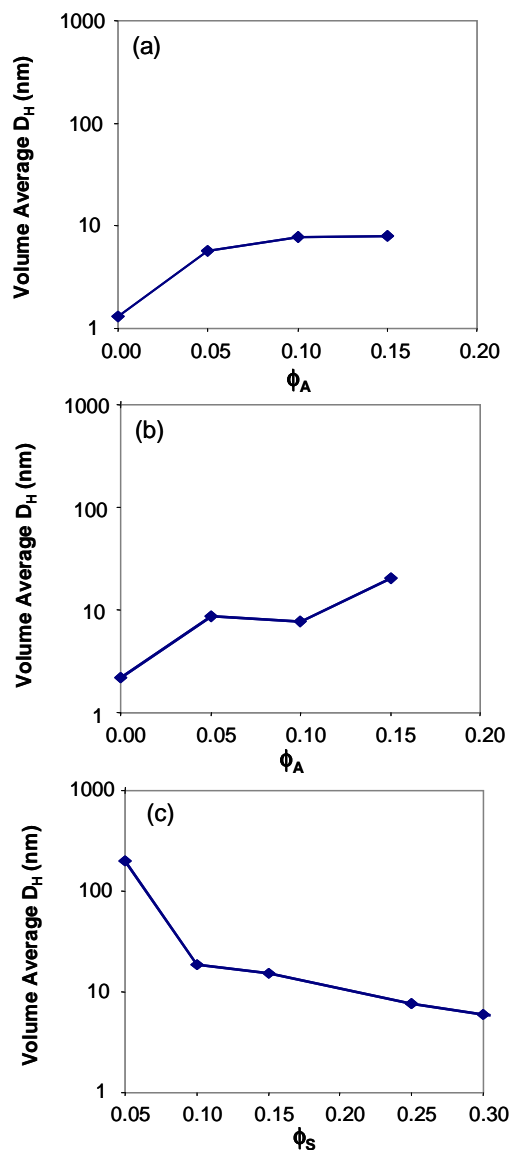
### A. Microemulsion Phase Behavior

Fig. 1 depicts the ternary diagram obtained from our rapid screening approach, which agrees remarkably well with the one in the literature obtained by multiple cloud point titrations [20]. DLS results (Fig. 2) obtained at select ternary compositions confirm reverse microemulsion (RM) existence throughout the region of optical transparency. As the aqueous concentration increases at constant concentrations of surfactant (Fig. 2a) and oil (Fig. 2b), the dispersed phase progresses from reverse micelles to larger water-swollen reverse micelles until finally a turbid multi-phase region is obtained. As the surfactant concentration increases at a constant aqueous concentration (Fig. 2c), the system transitions from a kinetically stabilized reverse emulsion toward a RM containing droplets of decreasing diameter. In addition, the phase prism results (Fig. 3) show that the RM existence field expands as temperature increases to contain upwards of 30% water by volume, an important factor when trying to maximize the yield of particles per volume of oil and surfactant.

As can be seen from Figs. 4-5, the RM existence field diminishes upon addition of dextran in a concentration-



**Fig. 1.** Pseudo-ternary diagram constructed using rapid screening procedure for a mixture of water, surfactant (3:2 w/w Span 80/Tween 80), and oil (3:1 w/w Captex 355/Capmul MCM). Absorbance at  $\lambda = 450$  nm:  $\square \leq 0.25$ ,  $\square \leq 0.50$ ,  $\square \leq 0.75$ ,  $\square \leq 1.00$ ,  $\square \leq 1.25$ ,  $\square \leq 1.50$ ,  $\blacksquare > 1.50$ .



**Figure 2.** Dynamic Light Scattering (DLS) results for select pseudo-ternary compositions as a function of water volume fraction ( $\phi_A$ ) at (a) constant surfactant volume fraction ( $\phi_S = 0.25$ ) and (b) constant oil volume fraction ( $\phi_O = 0.65$ ), and (c) as a function of surfactant volume fraction ( $\phi_S$ ) at constant water volume fraction ( $\phi_A = 0.10$ ).

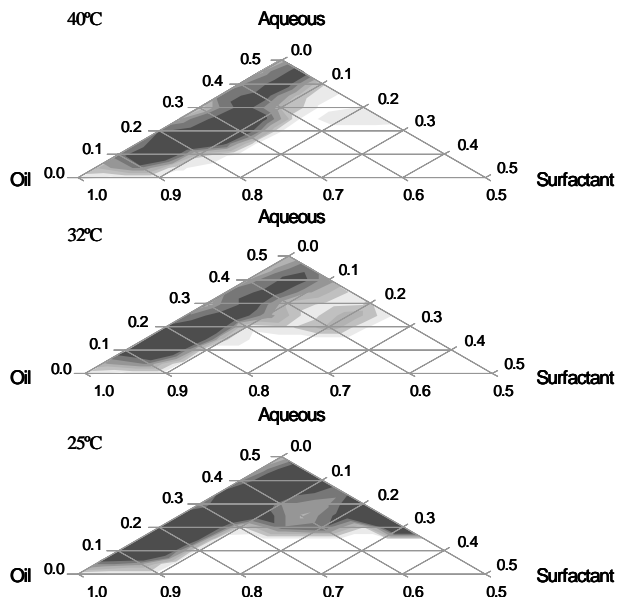


**Fig. 3.** Temperature dependent pseudo-ternary prism for a mixture of water, surfactant (3:2 w/w Span 80/Tween 80), and oil (3:1 w/w Captex 355/Capmul MCM).

Absorbance at  $\lambda = 450$  nm:  $\square \leq 0.25$ ,  $\square \leq 0.50$ ,  $\square \leq 0.75$ ,  
 $\square \leq 1.00$ ,  $\square \leq 1.25$ ,  $\square \leq 1.50$ ,  $\blacksquare > 1.50$ .

dependent manner, and as the MW increases from 10,000 to 70,000 g/mol, the existence field diminishes further. Other researchers have studied the effects of the water-soluble polymer, polyoxyethylene (POE), on RM phase behavior using ionic AOT/H<sub>2</sub>O/paraffin and nonionic C<sub>12</sub>E<sub>5</sub>/H<sub>2</sub>O/paraffin systems and found that the polymer may induce droplet cluster formation leading to, in some cases, macroscopic phase separation [21]. They also found that this effect was more

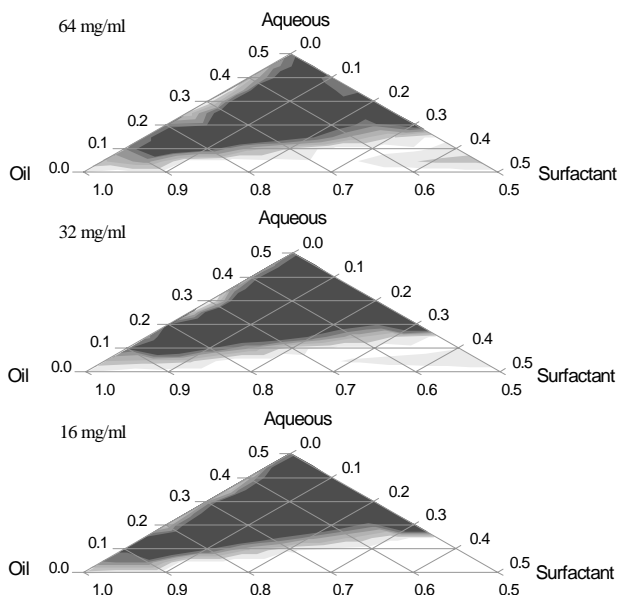


**Fig. 4.** Concentration dependence of dissolved dextran on reverse microemulsion phase behavior. Dextran MW = 10,000 g/mol.

Absorbance at  $\lambda = 450$  nm:  $\square \leq 0.25$ ,  $\square \leq 0.50$ ,  $\square \leq 0.75$ ,  
 $\square \leq 1.00$ ,  $\square \leq 1.25$ ,  $\square \leq 1.50$ ,  $\blacksquare > 1.50$ .

prevalent at higher polymer concentrations and higher MW. Possible explanations for this behavior include a polymer-induced increase in droplet attractive interactions or a tendency to maximize chain entropy by forming larger-sized water pools.

The effect of dissolved proteins on RM phase behavior was determined using a 0.1 N HCl aqueous phase. Insulin has minimal effect on the RM existence region as compared to the control (Fig. 6), while Con A exhibits two distinct regions of optical clarity separated by a turbid region at high surfactant, moderate oil concentrations (Fig. 7). In neutral pH buffered saline solutions, Con A and insulin induce a transition from transparency to turbidity as determined by ternary diagrams and DLS results (results not shown). Possible explanations include pH-dependent differences in protein charge, state of aggregation, and tertiary structure. For example, both Con A and insulin form tetramers and hexamers respectively at neutral pH, which may result in decreased solubility in the RM aqueous domains and increased droplet aggregation, similar to the effect observed for dextran. In addition, other researchers have observed large structural changes when proteins are added to reversed micelles as was the case, for instance, with cytochrome *c*, which enhanced percolation due to increase of attractive interactions between reversed micelles [22]. In our system, these attractive interactions are minimized at low pH but increase upon neutralization.

Based on the RM stability studies, we chose for particle synthesis the ternary composition ( $\phi_A : \phi_O : \phi_S = 10:65:25$ ) as it was found to yield the most stable RM for all three components over the concentration ranges of interest. In addition, based on the pH-dependent protein stability, the RM was formulated at low pH followed by neutralization to induce Con A crosslinking and nanoparticle formation.

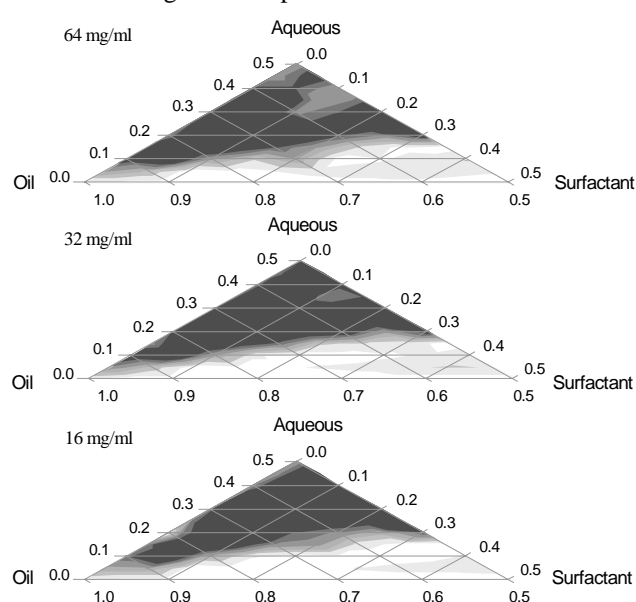


**Fig. 5.** Concentration dependence of dissolved dextran on reverse microemulsion phase behavior. Dextran MW = 70,000 g/mol.

Absorbance at  $\lambda = 450$  nm:  $\square \leq 0.25$ ,  $\square \leq 0.50$ ,  $\square \leq 0.75$ ,  
 $\square \leq 1.00$ ,  $\square \leq 1.25$ ,  $\square \leq 1.50$ ,  $\blacksquare > 1.50$ .

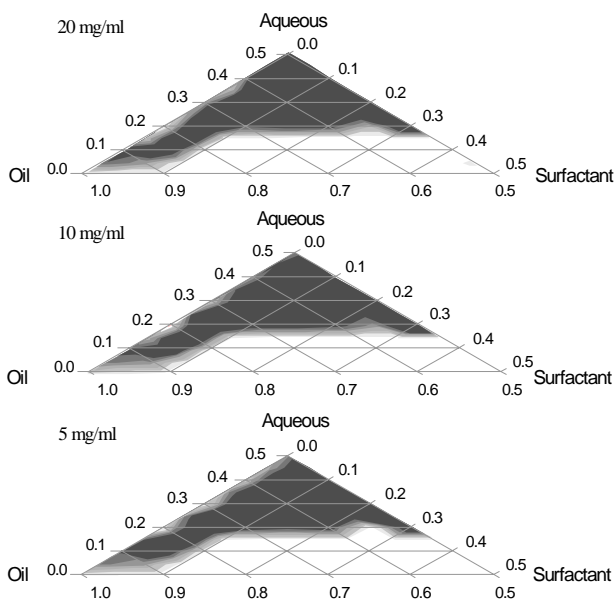


**Fig. 6.** Concentration dependence of  $\text{Zn}^{2+}$ -free bovine insulin on reverse microemulsion phase behavior using a 0.1 N HCl aqueous phase.

Absorbance at  $\lambda = 450$  nm:  $\square \leq 0.25$ ,  $\square \leq 0.50$ ,  $\square \leq 0.75$ ,  $\square \leq 1.00$ ,  $\square \leq 1.25$ ,  $\square \leq 1.50$ ,  $\blacksquare > 1.50$ .

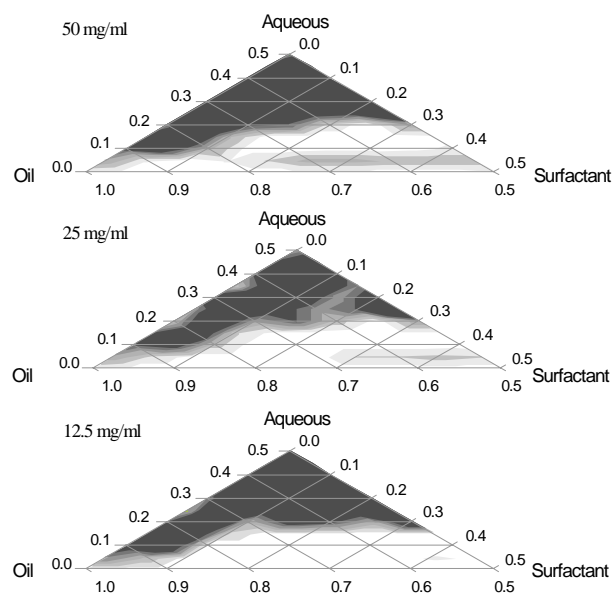
### B. Particle Characterization

Fig. 8 is a SEM micrograph of particles obtained from a formulation comprising FITC-Dex (MW = 280,000), [FITC-Dex] = 8 mg/ml, and [Con A] = 50 mg/ml. In this RM system, the particles obtained are much larger than the original aqueous domains, most probably due to the pH-dependent change in microemulsion phase behavior. In addition, one would expect that the interaction between Con A and dextran increases droplet attraction leading to particle growth. The entire population of particles is present in the submicron range, demonstrating our ability to restrict the reaction size domain and form physically crosslinked nanoparticles via RM-mediated synthesis.

### C. Dextran Crosslinking Efficiency

Fig. 9 illustrates the amount of crosslinked FITC-Dex versus the amount loaded into the RM for each of three [Con A]. First, both FITC-Dex MW = 40,000 g/mol (FITC-Dex 40) and FITC-Dex MW = 280,000 (FITC-Dex 280) demonstrate a strong dependence of the amount of crosslinking on [Con A]. The results show that as [FITC-Dex 40] decreases at a constant [Con A], the extent of crosslinking increases and reaches a maximum at [Con A]/[Dex]  $\sim$  3. At such high [FITC-Dex 40], it appears that there may be an excess of glucose ligands available for binding, resulting in soluble Con A-dextran complexes rather than insoluble particles.

The amount of crosslinked polymer may be improved by a factor of 5 by increasing the FITC-Dex MW to 280,000 g/mol. In addition, maximal crosslinking occurs at a lower [Con A]/[Dex] ratio. This can be explained by the fact that higher MW polymers require a fewer number of interpolymer crosslinks to form a sufficiently insoluble complex. The



**Fig. 7.** Concentration dependence of Con A on reverse microemulsion phase behavior using a 0.1 N HCl aqueous phase.

Absorbance at  $\lambda = 450$  nm:  $\square \leq 0.25$ ,  $\square \leq 0.50$ ,  $\square \leq 0.75$ ,  $\square \leq 1.00$ ,  $\square \leq 1.25$ ,  $\square \leq 1.50$ ,  $\blacksquare > 1.50$ .

FITC-Dex 40 system, on the other hand, most likely consists of a large number of branched, soluble Con A-Dex complexes with a small percentage of insoluble particles.

Mannosylation of FITC-Dex 40 (Man-Dex 40) also results in a greater extent of crosslinking over a range of [Con A]/[Dex] ratios and decreases the dependence of crosslinking on [Con A]. The higher affinity of Con A for mannose ( $K_{d,\text{glucose}} = 3.8K_{d,\text{mannose}}$ ) [23] ensures a higher proportion of bound polymer at a given concentration of Con A and dextran. In addition, mannosylation of the dextran backbone effectively increases the degree of branching, which is known to facilitate the precipitation reaction between Con A and  $\alpha$ -1,6-linked polysaccharides [24].

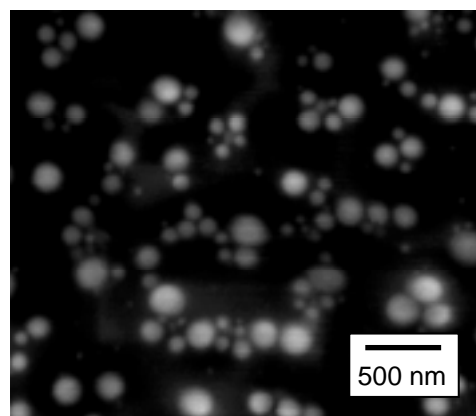


**Fig. 8.** Scanning electron micrograph of particles obtained via RM-mediated nanoparticle synthesis (FITC-Dex MW = 280,000 g/mol, [FITC-Dex] = 8 mg/ml, [Con A] = 50 mg/ml).

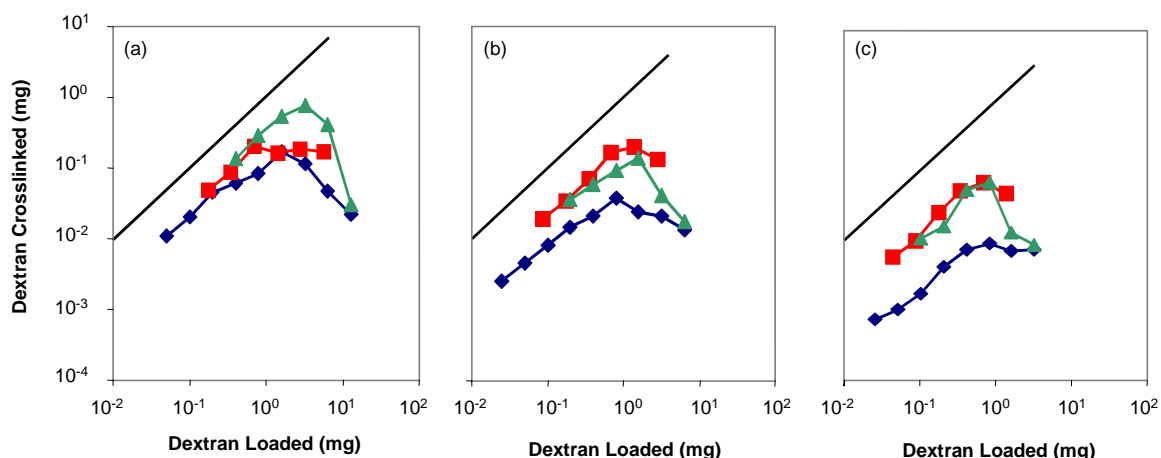


**Fig. 9.** Dextran crosslinked versus the amount loaded into the microemulsion for (◆) FITC-Dex 40, (▲) FITC-Dex 280, and (■) Man-Dex 40 at Con A = (a) 50 mg/ml, (b) 25 mg/ml, and (c) 12.5 mg/ml. The  $y = x$  line is included to represent 100% crosslinking efficiency.

#### D. Particle Dissolution and Insulin Release

Fig. 10 shows particle dissolution (experiment – control) as a function of both glucose concentration and the initial FITC-Dex 40 used in the particle synthesis and demonstrates glucose-sensitivity in all formulations particularly in the physiological hyperglycemic range of 1-10 mg/ml. The extent of dissolution is directly related to the crosslinking efficiency for each formulation.

Plotting the fraction of dextran dissolved as a function of glucose concentration for the FITC-Dex 280 (Fig. 11) shows that glucose-sensitivity may be controlled based on the relative ratio of Con A to polymer. Increasing the  $[\text{Con A}]/[\text{FITC-Dex 280}]$  from 1.6 to 6.3 results in particles that are more sensitive to higher glucose concentrations.

Finally, Fig. 12 depicts glucose-sensitive (experiment – control) insulin release for particles synthesized from FITC-Dex 40. The amount of insulin encapsulated and eventually released is determined by the extent of dextran crosslinking. In addition, the amount released as a function of glucose concentration correlates well with the extent of glucose-

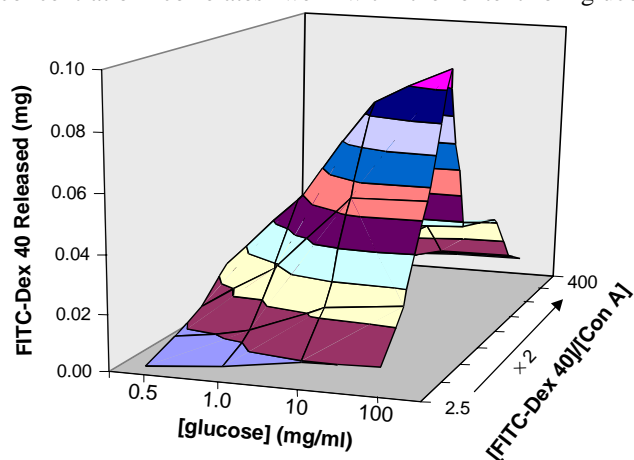


**Fig. 10.** Particle dissolution (experiment – control) as a function of glucose concentration and initial  $[\text{FITC-Dex}]/[\text{Con A}]$ . Particles are synthesized using an aqueous phase comprised of FITC-Dex 40 with  $[\text{Con A}] = 50$  mg/ml.

sensitive particle dissolution. The results are promising, but improvements are required to increase the extent of crosslinking and the corresponding insulin encapsulation and release.

#### IV. CONCLUSIONS

The phase behavior of biocompatible reverse microemulsions has been determined in the presence of dissolved polymers and proteins using a novel rapid screening technique developed in our laboratory. Future work will focus on detailed light scattering and conductivity measurements to further characterize the RM structural changes induced by the various macromolecules. In addition, determining the dependence of such structural changes on macromolecule size, charge density, and hydrophobicity as well as surfactant and oil properties may lead to a better understanding of the mechanism and a means for controlling the particle size.

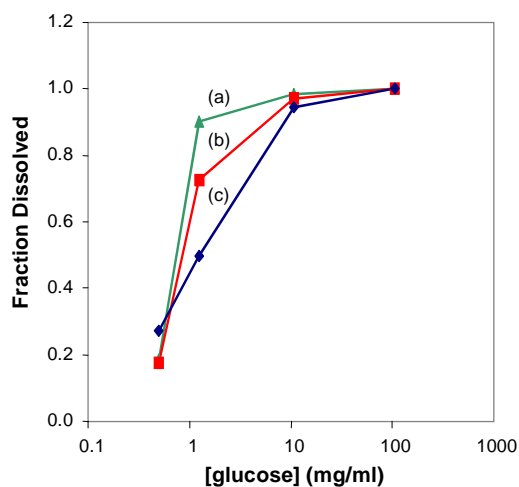


**Fig. 11.** Fraction of FITC-Dex 280 dissolved as a function of glucose concentration. Particles synthesized from an aqueous phase consisting of  $[\text{Con A}] = 50$  mg/ml with  $[\text{Con A}]/[\text{FITC-Dex 280}] =$  (a) 1.6, (b) 3.1, and (c) 6.3.

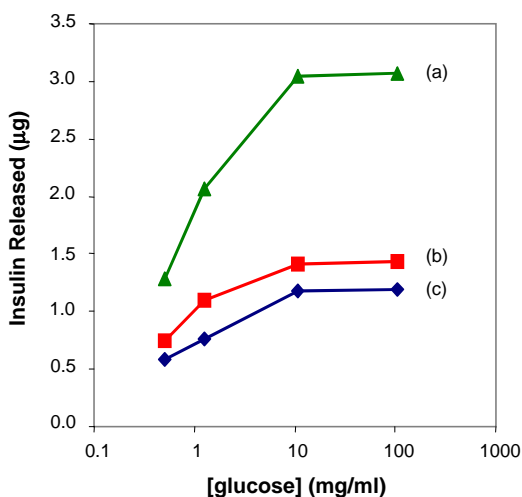


**Fig. 12.** Cumulative insulin release (experiment – control) versus glucose concentration. Particles synthesized from an aqueous phase consisting of FITC-Dex 40 and [Con A] = 50 mg/ml with [Con A]/[FITC-Dex 40] = (a) 0.4, (b) 0.8, and (c) 1.6.

The results from this study demonstrate the feasibility of synthesizing glucose-responsive nanoparticles based on RM-mediated crosslinking between dextran and Con A. The efficiency of Con A-dextran crosslinking and insulin encapsulation may be controlled by both the polymer molecular weight and dextran mannosylation. Furthermore, the glucose sensitivity of the nanoparticles may be manipulated by tailoring the Con A/dextran ratio.

As with the analogous macroscopic systems based on competitive binding, more work is required to precisely manipulate the glucose sensitivity and insulin release rates. The need to sufficiently immobilize insulin becomes more important as the size of the system and resulting diffusion time scales diminish. Potential solutions to this problem include (i) increasing polymer hydrophobicity to reduce swelling in aqueous media, (ii) covalent crosslinking to reduce particle mesh size and swelling, and (iii) glycosylation with higher affinity sugars to increase the density and strength of glucose-sensitive crosslinking.

As mentioned before, the Con A/dextran system was chosen as a model to develop the techniques required for nanoparticle synthesis. There is, however, concern over the immunogenicity and toxicity of the plant lectin Con A [25]. However, Taylor and coworkers have shown that covalent coupling of Con A to the polymer significantly reduces its leakage from glucose-sensitive hydrogel membranes. In addition, precise covalent crosslinking of the particles may prevent Con A release while still enabling glucose-sensitive insulin release [14]. Finally, evaluating the performance of less toxic glucose-binding proteins (e.g. lectins isolated from the fava bean or garden pea) in these systems may result in a potentially safer and more applicable nanoparticulate insulin delivery system.

#### ACKNOWLEDGMENT

The authors thank A. G. Garratt-Reed (MIT CMSE) for his assistance in SEM studies and Prof. T. A. Hatton's laboratory (MIT Department of Chemical Engineering) for the assistance with DLS measurements.

#### REFERENCES

- [1] G. P. Carino, J. S. Jacob, E. Mathiowitz, *J. Control. Release* **65**, 261-269 (2000).
- [2] E. Mathiowitz, *et al.*, *Nature* **386**, 410-414 (1997).
- [3] A. K. Andrianov, L. G. Payne, *Adv. Drug Deliv. Rev.* **34**, 155-170 (1998).
- [4] S. Watnasirichaikul, T. Rades, I. G. Tucker, N. M. Davies, *J. Pharm. Pharmacol.* **54**, 473-480 (2002).
- [5] H. M. Chen, R. Langer, *Adv. Drug Deliv. Rev.* **34**, 339-350 (1998).
- [6] A. T. Florence, A. M. Hillery, N. Hussain, P. U. Jani, *J. Control. Release* **36**, 39-46 (1995).
- [7] D. T. Ohagan, *J. Anat.* **189**, 477-482 (1996).
- [8] K. Stahl, M. Claesson, P. Lilliehorn, H. Linden, K. Backstrom, *Int. J. Pharm.* **233**, 227-237 (2002).
- [9] M. C. Garnett, *et al.*, *MRS Bull.* **24**, 49-56 (1999).
- [10] M. Brownlee, A. Cerami, *Science* **206**, 1190-1191 (1979).
- [11] J. Kost, R. Langer, *Adv. Drug Deliv. Rev.* **46**, 125-148 (2001).
- [12] T. Miyata, T. Urugami, K. Nakamae, *Adv. Drug Deliv. Rev.* **54**, 79-98 (2002).
- [13] A. A. Obaidat, K. Park, *Biomater.* **18**, 801-806 (1997).
- [14] S. Tanna, T. Sahota, J. Clark, M. J. Taylor, *J. Drug Target.* **10**, 411-418 (2002).
- [15] A. J. Zarur, J. Y. Ying, *Nature* **403**, 65-67 (2000).
- [16] R. Mehvar, *J. Control. Release* **69**, 1-25 (2000).
- [17] L. A. Sluyterman, *Biochim. Biophys. Acta* **17**, 223-236 (1955).
- [18] R. Ballerstadt, J. S. Schultz, *Anal. Chim. Acta* **345**, 203-212 (1997).
- [19] M. J. Lawrence, G. D. Rees, *Adv. Drug Deliv. Rev.* **45**, 89-121 (2000).
- [20] S. Watnasirichaikul, N. M. Davies, T. Rades, I. G. Tucker, *Pharm. Res.* **17**, 684-689 (2000).
- [21] A. M. Bellocq, *Langmuir* **14**, 3730-3739 (1998).
- [22] C. A. T. Laia, W. Brown, M. Almgren, S. M. B. Costa, *Langmuir* **16**, 465-470 (2000).
- [23] J. N. Sanders, S. A. Chenoweth, F. P. Schwarz, *J. Inorg. Biochem.* **70**, 71-82 (1998).
- [24] I. J. Goldstein, C. E. Hollerman, J. M. Merrick, *Biochim. Biophys. Acta* **97**, 68-76 (1965).
- [25] T. L. Li, H. B. Lee, K. Park, *J. Biomater. Sci.-Polym. Ed.* **9**, 327-344 (1998).